Article

Assesment of Satellite and Radar Quantitative Precipitation Estimates for Real Time Monitoring of Meteorological Extremes Over the Southeast of Iberian Peninsula

Fulgencio Cánovas-García [1,†]*, Sandra García-Galiano [1,†] and Francisco Alonso-Sarría [2,†]

[1] Unidad Predepartamental de Ingeniería Civil, Universidad Politécnica de Cartagena, Paseo Alfonso XIII, 52. 30203 Cartagena, Spain
https://www.researchgate.net/profile/Fulgencio_Canovas-Garcia

[2] Instituto Universitario del Agua y Medio Ambiente, Universidad de Murcia. Edificio D, Campus de Espinardo, s/n, 30001 Murcia, Spain

* Correspondence: fulgencio.canovas@upct.es

† These authors contributed equally to this work.

Abstract: QPEs (Quantitative Precipitation Estimates) obtained from remote sensing or ground-based radars could complement or even be an alternative to rain gauge readings. However, to be used in operational applications, a validation process has to be carried out, usually by comparing their estimates with those of a rain gauges network. In this paper, the accuracy of two QPEs are evaluated for three extreme precipitation events in the last decade in the southeast of the Iberian Peninsula. The first QPE is PERSIANN-CCS, a satellite-based QPE. The second is a meteorological radar with Doppler capabilities that works in the C band. Pixel-to-point comparisons are made between the values offered by the QPEs and those obtained by two networks of rain gauges. The results obtained indicate that both QPEs were well below the rain gauge values, especially in extreme rainfall time slots. There seems to be a weak linear association between the value of the discrepancies and the precipitation value of the QPEs. The main conclusion is that neither PERSIANN-CCS nor radar, without empirical calibration, are acceptable QPEs for the real-time monitoring of meteorological extremes in the southeast of the Iberian Peninsula.

Keywords: Quantitative Precipitation Estimates; Validation; PERSIANN-CCS; meteorological radar; Satellite Rainfall Estimates

1. Introduction

Precipitation is a highly relevant feature in Earth sciences. Precipitation estimations with good spatial and temporal resolution are important in hydrology, climate research [1], ecology

Peer-reviewed version available at Remote Sens. 2018, 10, 1023; doi:10.3390/rs10071023

and meteorology. Precipitation estimations might be the most important meteorological input for calibrating and using hydrological and ecological models [2].

In much of the planet, weather networks are not dense enough to obtain information suitable for water resources management or to provide an adequate response to disasters due to extreme weather events. Moreover, in such areas water resources are crucial to maintain large human populations and fragile or threatened ecosystems. In developing countries and in difficult to access places, weather networks are especially scarce, so that spatial estimations of precipitation become particularly uncertain [3]. Moreover, the temporal resolution of rain gauges in these stations is daily or even less frequently, so this information hardly serves to monitor extreme weather events.

Meteorological radars have been used for flood warnings, but they are very expensive to set up and maintain, and their coverage is limited in mountainous areas [4]. In fact, the first operational network of meteorological radars in tropical mountain areas has only been operational for a few years [5]. These authors and Nikolopoulos et al. 2013 [6] also identified the difficulty of maintaining radar networks in developing countries. This lack of adequate data for precipitation monitoring limits the scope for hydro-meteorological research and the use of physical or statistical models for water resources management [7].

Rain gauge networks have been used as primary source of rainfall estimates for over a century. However, while these devices provide direct and accurate (relative to other sensors) rainfall estimations, they are associated with small sampling areas [6]. Such estimations have traditionally been considered as ground truth. However, several problems have been described [8]: record alterations by natural or human-induced disturbances, spillage of collected precipitation while the tipping bucket is in motion during heavy rainfall events, or wind and eddy effects. In the case of snow or very strong winds, these errors may be substantial and should initially be considered, although a quantitative correction is almost impossible [2]. Another problem arises when using rain gauges as a source of information of precipitation: rain gauges perform point specific measurements and, even in very dense networks, it may not be possible to capture the spatial variability of precipitation, especially when working at subhour scales [9] or when dealing with very localised convective or orographic precipitation. For example, Michaud and Sorooshian (1994) [10] estimated that the suitable density for measuring convective rainfall in medium-sized semi-arid basins is around one rain gauge every 4 km^2, a density far greater than the density existing in the study area of this research, even superimposing all the existing networks. Such a density can only be reached in experimental basins.

The QPEs (Quantitative Precipitation Estimates) obtained by remote sensing can complement or be considered an alternative to rain gauge measurements. Satellite-based QPE are valuable continuous records on several temporal [11] and spatial scales. At present, such satellite rainfall products

Peer-reviewed version available at Remote Sens. 2018, 10, 1023; doi:10.3390/rs10071023

present three characteristics that would be of potential use for environmental applications: close to global coverage (all longitudes and latitudes between 60°N and 60°S), sufficiently long for climatic applications (at least 30 years) and, finally, independence from the adverse conditions when the area is affected by extreme events. Satellite-based QPEs can provide acceptable good estimations of precipitation in "un-gauged" regions, such as oceans, hard-to-reach mountainous areas or deserts [2]. We agree with Zambrano-Bigiarini *et al*. (2017) [12] that satellite-based QPEs provide an unprecedented opportunity for a wide variety of meteorological and hydrological applications.

Several satellite-based QPEs are available, such as PERSIANN-CDR (Precipitation Estimation from Remotely Sensed Information using Artificial Neural Networks-Climate Data Record), PERSIANN-CCS (Cloud Classification System), CMORPH (Climate Prediction Center Morphing technique), TRMM Multi-satellite Precipitation Analysis (TMPA) 3B42RT and 3B42V6 dataset, among others [13]. As well as the more recently released Multi-Sensor Precipitation Estimate of EUMETSAT (European Organisation for the Exploitation of Meteorological Satellites), or the wide dataset of products from Precipitation Measurement Missions.

In recent decades, the frequency of flood disasters in Europe has increased [14]. In Spain, floods are the natural hazard with the greatest territorial impact and are responsible for great socio-economic looses [15]. Spain is also the EU country most affected by flash floods [14]. In the southeast of the Iberian Peninsula these phenomena have caused a very high number of deaths and millions of economic losses. Recent examples are the three events analysed in section 2.2.

It is not possible to gauge all small and medium sized basins, or larger hydrological systems that may produce a flooding event to measure runoff in the channels, so precipitation intensity remains the most used source of information during extreme weather events. So, regardless of the methodology or type of modelling used, warning accuracy will depend on the accuracy of the precipitation estimation [6]. Serrano Notivoli et al. (2017) [16] developed a high resolution daily precipitation grid for the whole of Spain. They also analysed the estimation uncertainties, concluding that the highest uncertainty values appear in SE Spain, the study area of this paper. The reason is that most of the precipitation in this area is produced by convective systems generated over the Mediterranean Sea interacting with Potential Vorticity Streamers (PVS) or cut-offs in the higher troposhere. In such conditions, the entrance of wet air masses to the land is driven by the relief pattern and the wind direction. The interaction of both factors produces highly localised upwinds and a very irregular precipitation pattern that are very difficult to estimate interpolating with daily rain gauge data alone. This is obviously a considerable handicap for hydrological forecasting.

Satellite-based QPEs have not been well integrated into operational and decision-making applications because of the lack of rigorous validation and uncertainty analysis [17]. Hong *et al*.

(2007) [8] pointed out that the strong spatio-temporal variability of precipitation makes it necessary to rigorously assess QPE accuracy before the estimates can be used with confidence. In a very recent paper, Zambrano-Bigiarini *et al*. (2017) [12] claimed that no satellite-based QPE can be generally considered more accurate than any others on a daily scale, and that accuracy must be assessed on a case-by-case basis in the study area in question.

At the moment, the most common way of estimating this accuracy is to compare QPEs with rain gauge and meteorological radar data. Accuracy estimations of global products such as PERSIANN-CCS in in areas where rain gauge data is available might be useful to estimate if they are accurate enough to be used in areas where rigurous validation is impossible due to the absence of rain gauge information with which to compare satellite-based QPEs.

The aim of this research was to evaluate the accuracy of two precipitation products during heavy rainfall events. The intention was also to ascertain whether any of the QPEs could be regarded as a good substitute for the information provided by a rain gauge if it malfunctions. We have compared precipitation estimations of two rain gauge networks with those estimated by a satellite-based QPE (PERSIANN-CCS) and a ground-based QPE (meteorological radar) during the three most important heavy rainfall episodes recorded during the last ten years in the southeast of the Iberian Peninsula (Spain). Comparisons are made with aggregated data, using statistics for the entire study area and for the most affected river basins, on the one hand, and in a disaggregated manner, doing the same for the rain gauge that recorded the greatest accumulations and intensities of precipitation, on the other. The comparisons are made on a spatial basis, using interpolation to map the differences in accumulated precipitation and maximum hourly intensity between the two QPEs and the rain gauges on the one hand, and between the two QPEs, on the other. Comparisons are also made with a temporal perspective using statistics on the agreement among precipitation estimations calculated on an hourly scale.

2. Materials and Methods

2.1. Study area

The research was carried out in the terrestrial portion of the Segura River Basin District, located in south-eastern Spain (Figure 1), with a surface area of 18,740 km^2 covering the Segura River basin and other small coastal basins [18]. It is a territory with scarce and irregular rainfall, high temperatures and a high annual number of hours of sun. There is a NW-SE precipitation gradient that ranges from approximately 1000 mm/year in the headwaters of the Segura river to less than 300 mm/year in the coastal zone [19]. With the exception of the Segura river, the most common channels are ramblas (ephemeral rivers), frequently responsible for flash floods [15]. Although it is one of the smallest

Preprints (www.preprints.org) | NOT PEER-REVIEWED | Posted: 9 May 2018 doi:10.20944/preprints201805.0150.v1

Peer-reviewed version available at Remote Sens. 2018, 10, 1023; doi:10.3390/rs10071023

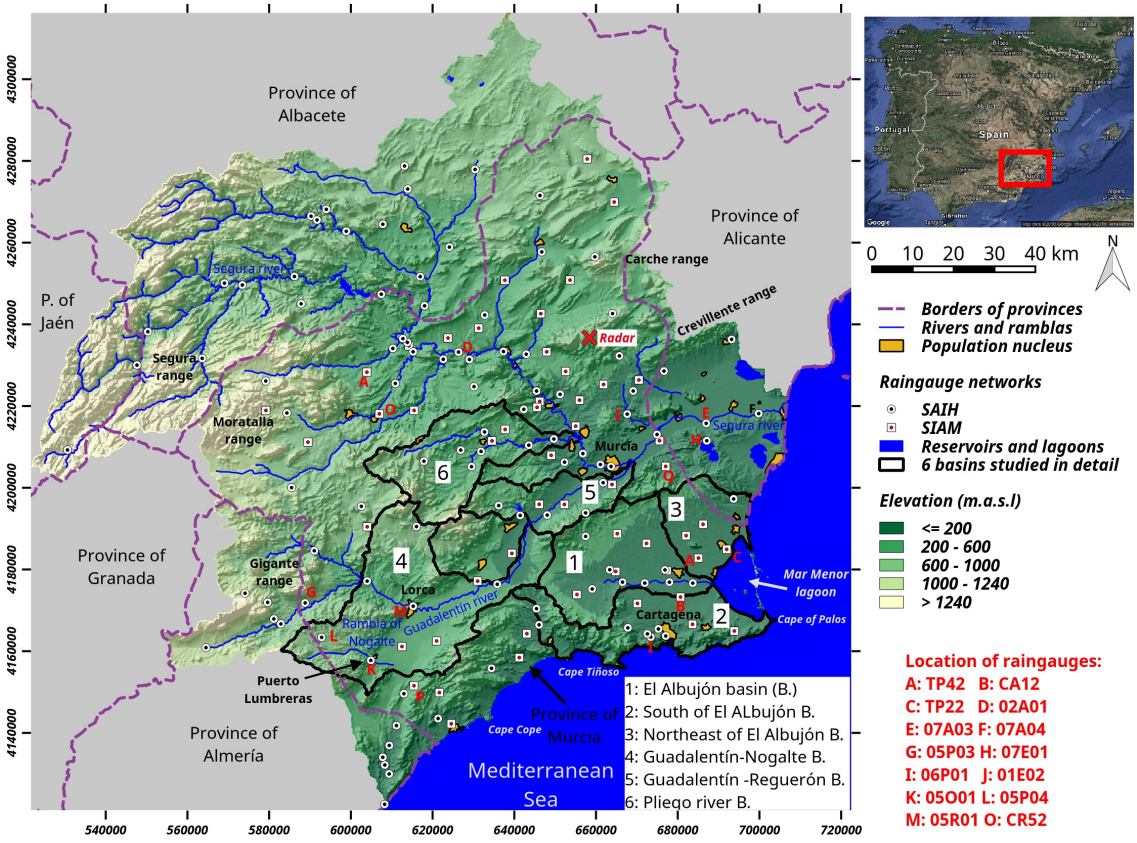

Figure 1. Map of the study area, the Segura River Basin District. Coordinate Reference System is ETRS89 with proyected coordinates (EPSG code: 25830).

basins in Europe, its management is quite complex as a result of having water resources from different sources (surface and groundwater resources, desalination, transfers and reuse) and multiple uses that compete for the scarce water resources [20].

2.2. Rainfal events

Three very intense precipitation events in the last decade were identified and characterized. The first one took place on 27-28 September, 2009 and affected the Campo of Cartagena area. A PVS, scarcely visible in surface, reached the Gulf of Cadiz with a divergence zone near the southeast of the study area. In surface, the situation was characterized by easterly winds that reached the study area after a long journey over the Mediterranean Sea in which the air mass charged sensible and latent heat and moisture. The confluence of this warm and wet air with a cold vortex in air generated a high lapse rate and strong instability. In addition, on the 28^{th}, a polar continental air mass reached the Iberian Peninsula from the northeast increasing the convectivity and producing strong precipitation, especially near the coast. As two examples, the 06P03 rain gauge, located about 5 km NW of La Vaguada, recorded 199 mm in 29 hours and the CA12 rain gauge, located in La Palma, recorded 268

Peer-reviewed version available at Remote Sens. 2018, 10, 1023; doi:10.3390/rs10071023

Figure 2. The rambla of Nogalte is normally dry (a) and only runs water when there is heavy rainfall in the upper basin as on the 2012/09/28 event (b). Sources: a) [21], b) CHS, 2013.

mm in 30 hours. The two mentioned rain gauges were located in the municipality of Cartagena, and the rainfall produced several flash floods in the Campo de Cartagena basins (basins number 1, 2 and 3 in Figure 1).

The second event occurred during the first half of 28 September, 2012. In this case a deep PVS reached Madeira Island on September the 26^{th} and moved to the east, eventually breaking to form a cut-off southwest of the Iberian Peninsula. At the same time, warm air from North Africa reached the Iberian Peninsula generating a warm front feeding the convective systems with warm, moist and unstable air. Substantial rainfall occurred in the overlapping area of the upper-level anomaly and the lower levels advection. A quasi-stationary mesoscale convection system lasted several hours over Murcia. The rain gauge 05P03, located in the foothills of Sierra del Gigante (Municipality of Lorca), recorded 124 mm in five hours and the 05O01 rain gauge, located in Puerto Lumbreras, recorded 153 mm in six hours. Massive flash floods were registered in the Nogalte (Figure 2) and Guadalentín basins (basin number 4 in Figure 1).

The most recent event was registered between 17 and 19 December 2016, and was the most important meteorological episode of the whole year for the Iberian Peninsula. On 16 December 2016, a PVS visible both in surface and in the 500 hPa topography began to form and move towards The Gulf of Cadiz and western Morocco eventually forming a cut-off located over Morocco that drove southeastern winds towards SE Spain with a clear divergence in the study area. This cut-off was quite stationary. In surface, an E-SE flow, due to a high pressure cell in Europe and a low pressure cell in Africa, affected the study area, driving moist air to the coast and generating high instability. The highest rainfall intensities were registered in Campo of Cartagena and the east coast of the study area, where the rainfall exceeded 50 mm in one hour in the Torre Pacheco and San Javier rain gauges. Areas close to the Mar Menor lagoon, which environment has undergone a strong process of global transformation due to tourist [22] and farming activity, were severely affected by the storm and the consequent flooding.

Peer-reviewed version available at Remote Sens. 2018, 10, 1023; doi:10.3390/rs10071023

2.3. Satellite-based QPE: PERSIANN-CCS

PERSIANN-CCS [1] is a system based on satellite imagery and pattern recognition techniques applied for the automatic classification of several types of clouds in order to estimate the rainfall in each pixel.

PERSIANN-CCS produces non-empirical adjusted QPEs with a time resolution of one hour, a spatial resolution of 0.04° ($\approx 4 \times 4\ km^2$ in Spanish latitudes), with near to global coverage (between 60°N and 60°S) and a lag time of approximately one hour (near-real time), characteristics considered sufficient for hydrological applications at local scale [23]. Its coordinate reference system (CRS) is WGS84 with geodetic coordinates (EPSG code: 4326). Since PERSIANN-CCS is available in near-real time, it is suitable for use in flood warning and management applications [24,25], especially in large river systems such as the Segura or Guadalentín river basins where the one-hour temporal resolution has little impact on hydrological analysis compared to smaller flash floods prone basins [26]. Very promising advances have been made in the calibration of PERSIANN-CCS with data from other satellite data [27], but, unfortunately, these products are not available in near-real time.

2.4. Ground-based QPE: Meteorological Radar

Radar data from the Spanish Meteorology Service (AEMET) has been used. This apparatus operates in the C band (5.6 GHz) and is equipped with Doppler capability. It currently provides data for a circle of 240 km radius (long range mode) and provides images in Cartesian local projection according to Lambert's conformal conical centered on the radar (38.27º N, 1.19º W). Each image consists of 480 X 480 pixels and a spatial resolution of $1 \times 1\ km^2$ when operating in long-range mode. When working in short-range mode, it provides information for a circle area of 120 km radius and a spatial resolution of $500 \times 500\ m^2$. Hourly accumulated precipitation data, the QPE with highest temporal resolution offered by AEMET, were used in this work. Meteorological radar data is not freely accessible. An official request to AEMET is required and the price is 0.51 euros/image plus taxes, except when a discount for scientific research is approved by AEMET.

For the 2009 episode, hourly accumulation data, based on CAPPI (constant altitude plan position indicator), are available for working in short range mode. No meteorological radar data are available for the 2012 episode. Finally, for the 2016 episode, an hourly QPE called SRI (surface rainfall intensity) was used. This is an improved product that takes into account the nature of the precipitation (convective or stratiform) before applying, or not, a correction for the vertical reflectivity profile. Both the QPE CAPPI and the SRI estimate the precipitation intensity R in mm/h from $R(Z)$ ratios of type $Z = aR^b$, in which Z is the reflectivity factor in $mm^6\ m^{-3}$ and a and b are constants. The main advantage of

this QPE over a satellite-based QPE is a lag time of about 7 minutes from the end of the accumulation period, as shown in the image metadata.

2.5. Rain gauges

PERSIANN-CCS and radar data were compared with two rain gauge networks. The SIAM agro-meteorological network consists of several automatic rain gauges (45 in the 2009 event, 44 in the 2012 event and 47 in the 2016 event) with a temporal resolution of one hour. The second network is the SAIH-Segura (Automatic Hydrological Information System of the Segura River Basin) operated by the Water Authority (Segura Basin Hydrological Confederation, CHS). It had 64 rain gauges operative for the 2009 event, 66 for the 2012 event, and 106 for the 2016 event. The time resolution of this network is 5 minutes. The CRS of the two rain gauge networks is ETRS89/UTM zone 30N (EPSG code: 25830). Both networks were joined to obtain a more dense network. In 2009 and 2012 there was a rain gauge for every 173 km^2, for the 2016 event the density increased to a rain gauge every 124.5 km^2.

SIAM network data are evaluated and validated internally before being made available to the public. SAIH-Segura network data for the 2009 and 2012 events are reported in the system as "filtered and consolidated". Only for the 2016 event did the data appear at the time of the download as "provisional, obtained in real time without checking". Regardless of this, the precipitation data have been analyzed to eliminate possible erroneous values prior to comparison with the QPEs using the methodology proposed by Velasco-Forero *et al*(2009) [28]. Rain gauges with cumulative precipitation lower than 1.5 mm from the entire event were discarded from the analysis when the cumulative radar precipitation was more than 10 mm. In addition, long periods of inactivity of the rain gauges have been monitored to ensure that they correspond to the same pattern in the radar data. After the corresponding analyses, one rain gauge was removed from the SIAM network in the 2009 event and another one from the SAIH-Segura network in the 2016 event.

2.6. Assesssment of Quantitative Precipitation Estimates

As proposed by other authors [12,29–31] a point-to-pixel analysis was used to compare rain gauge data with the QPEs. The rain gauge layers were reprojected to the CRS of the QPE to avoid uncertainties associated with the resampling of the pixels, and when more than one rain gauge intersected with a QPE pixel, the mean value of the rain gauges was used for the comparison.

To implement a point-to-pixel comparison is a difficult task because of several uncertainties to be taken into account when evaluating the statistics derived from the comparison. For example, the spatial support of QPE and rain gauges is different. The rain gauge entrance (in all cases less than 0.05 m^2) can be approximated to a point measurement, while the values stored in the pixels of the QPEs correspond to averages over the volume of a grid cell [9]. This causes a smoothing of the QPEs'

values compared to the punctual estimates of the rain gauges [32]. Therefore, the differences in the values of rain gauges and QPE pixels are not only due to errors in the QPEs, but also to differences in spatial support [9]. This problem increases if the spatial resolution of the QPE is smaller, so the problem is much more serious for PERSIANN-CCS than for both radar images. In addition, the finescale variability of precipitation even at short distances, especially with convective precipitation, which cannot be represented by a dispersed network of rain gauges [8], introduces uncertainty into the precipitation values averaged over large areas.

Such problems require careful interpretation of the observed differences when a point-to-pixel comparison is applied. According to Schiemann *et al.* (2011) [9], accepting the assumption that the above effects lead to a random component in the pluviometer-QPE differences, comparisons made for a large number of rain gauges (such as that used in this research) can provide some guidance concerning the accuracy obtained by different QPEs. For these reasons, the word "error" is avoided as the word "difference" is considered more appropriate; although terms such as overestimate or underestimate (always using the rain gauge value as the baseline) are introduced with the intention of simplifying the text as much as possible.

The statistics calculated to report the degree of agreement among rain gauges and QPEs were: $diff_i = qpe_i - gau_i$, where gau_i was the estimated precipitation for a given rain gauge during a given time interval and qpe_i was the estimated precipitation for the QPE at the pixel intersecting with the location of the previous rain gauge for the same time interval; the average rainfall of rain gauges as $\overline{gau} = \frac{1}{n}\sum gau_i$; the average precipitation of the QPE, $\overline{qpe} = \frac{1}{n}\sum qpe_i$; the root mean square difference as $RMSD = \sqrt{\frac{1}{n}\sum diff_i^2}$; the mean absolute difference as $MAD = |\frac{1}{n}|diff_i|$; the bias as $bias = \frac{1}{n}\sum diff_i$; Pearson's linear correlation coefficient[33, page 134]; the relative MAD as $rMAD = \frac{MAD}{\overline{gau}}$ and the relative RMSD as $rRMSD = \frac{RMSD}{\overline{gau}}$.

Although these statistics may be appropriate for continuous simulation problems, when it comes to the analysis of extreme weather events it is necessary to carefully manage values close to zero. In very intense but very localised precipitations, the use of these statistics might produce misleading results since the values close to zero, if abundant, have a downward influence on the value of the statistic. In research such as this, the use of conditional statistics is desirable. In our case the condition was that either the rain gauge estimate (gau_i) or the QPE estimate (qpe_i) was equal to or greater than 1 mm/h. Conditional statistics are represented in this work with an asterisk in front of the statistic's name, so the conditional MAD is $*MAD$. Other authors [8,9,28,34] have also used conditional statistics, although there is no consensus neither concerning the logical operator ('AND' or'OR') or the threshold to be used. Although we believe that the use of conditional statistics is more appropriate, we also offer non-conditional statistics to facilitate comparison with other works.

The statistics were calculated for the study area, for the (two or three) sub-basins with the highest accumulated rainfall during each event, and for the three rain gauges with the highest accumulation recorded for each event and which were not located in the aforementioned sub-basins (Table 1).

Different comparisons were carried out to determine the degree of agreement between the three sources of information. A comparison of the estimated precipitation values at a given location was made (Figures 4 c, 5 d and e, 6 d, e and f, 7 e and f and Figures 13 and 14). Although the above comments on uncertainties in point-to-pixel comparisons should be borne in mind, it is always appropriate to obtain results without aggregation and for specific locations in the territory. A comparison of statistics has also been made for the course of the three storms in different spatial areas (Figures 5, 6 and 7). This allowed us to identify the QPE whose rainfall values were closest to those of the rain gauges and to relate the observed differences with the precipitation intensities estimated by the rain gauges. An analysis of the spatial distribution of the total accumulation of events and of the maximum hourly intensities has been carried out to compare the two QPEs and identify, for each of them, the places where the greatest differences with respect to rain gauges occured. Interpolation techniques were used for this purpose. Finally, a pixel-by-pixel comparison, as proposed by Nguyen *et al*. (2015) [26], between the radar and PERSIANN-CCS was carried out by generating a mapping of statistics and linear association between the two QPEs for the 2009 and 2016 events (Figure 12).

3. Results

3.1. Statistics

Table 1 shows the statistics of the degree of agreement and linear association among rain gauges and QPEs. The number of rain gauges may not be equal for the same event in the two QPEs analysed due to their different spatial resolutions; it is always lower in PERSIANN-CCS due to its lower spatial resolution. The observations column indicates the number of pairs of precipitation values taken into account to calculate the statistics. In all the events, the number of non-conditional observations in the study area more than doubles the conditional observations. These large differences in extreme precipitation events reflect their highly localised character. Focusing on the basin with the greatest accumulation of precipitation in the 2009 event (647 km^2), the number of conditional observations is approximately 72 percent less than the number of non-conditional observations. In the 2012 event, the percentage of conditional observations is less than 50 in the sub-basin with the greatest accumulation of precipitation.

In the September 2009 event (Table 1 a), the RMSD of the entire study area is moderate, 3.5 mm/h for PERSIANN-CCS and 2.9 mm/h for radar. However, this value is partly due to the high number of hours in which both PERSIANN-CCS and radar have precipitation values below 1. The

Preprints (www.preprints.org) | NOT PEER-REVIEWED | Posted: 9 May 2018 doi:10.20944/preprints201805.0150.v1

Peer-reviewed version available at Remote Sens. 2018, 10, 1023; doi:10.3390/rs10071023

Table 1. Statistics of agreement and linear association between raingauges and the corresponding pixels of PERSIANN-CCS and radar, for the three events in the three basins most affected by each event and selected raingauges.

(a) 2009, 27^{th} and 28^{th}, September Event

PERSIANN-CCS, spatial resolution $\approx 4 \times 4\,km^2$

Name	nº gau	Obs.	*Obs.	$\overline{qpe}$	*$\overline{qpe}$	$\overline{gau}$	*$\overline{gau}$	RMSD	*RMSD	rRMSD	*rRMSD	MAD	*MAD	rMAD	*rMAD	Bias	*Bias	R	*R	$\sum qpe$	$\sum gau$
S. Al	5	220	158	2.9	4.0	5.0	6.9	8.2	9.6	1.6	1.4	4.1	5.7	0.8	0.8	-2.1	-2.9	0.34	0.18	–	–
Al	6	264	193	3.0	4.0	2.9	3.9	5.1	6.0	1.8	1.5	3.3	4.5	1.1	1.1	0.1	0.1	0.22	0.04	–	–
NE. Al	5	220	155	3.2	4.5	2.6	3.7	5.6	6.7	2.1	1.8	3.9	5.4	1.5	1.5	0.6	0.8	0.07	-0.17	–	–
02A01	1	44	44	0.5	0.5	2.8	2.8	3.7	3.7	1.3	1.3	2.3	2.3	0.8	0.8	-2.3	-2.3	0.71	0.71	21	121
07A03	1	44	27	2.1	3.3	2.5	4.0	4.6	5.9	1.8	1.5	2.8	4.4	1.1	1.1	-0.4	-0.7	0.47	0.34	94	110
07A04	1	44	25	1.8	3.1	4.2	7.3	9.0	11.9	2.1	1.6	4.0	7.0	1.0	1.0	-2.4	-4.2	0.49	0.35	78	185
Total	**106**	**4664**	**2060**	**1.4**	**3.0**	**1.4**	**2.9**	**3.5**	**5.2**	**2.6**	**1.8**	**1.6**	**3.5**	**1.2**	**1.2**	**0.0**	**0.1**	**0.31**	**0.08**	**–**	**–**

Radar, CAPPI product in short range mode, spatial resolution $\approx 500 \times 500\,m^2$

Name	nº gau	Obs.	*Obs.	$\overline{qpe}$	*$\overline{qpe}$	$\overline{gau}$	*$\overline{gau}$	RMSD	*RMSD	rRMSD	*rRMSD	MAD	*MAD	rMAD	*rMAD	Bias	*Bias	R	*R	$\sum qpe$	$\sum gau$
S. Al	5	220	159	2.5	3.4	5.0	6.9	7.9	9.3	1.6	1.4	3.9	5.3	0.8	0.8	-2.5	-3.4	0.46	0.34	–	–
Al	6	264	168	1.8	2.8	2.9	4.5	4.2	5.2	1.4	1.2	2.2	3.4	0.8	0.8	-1.1	-1.7	0.49	0.31		–
NE. Al	5	220	110	1.2	2.3	2.6	5.1	4.6	6.5	1.8	1.3	2.4	4.6	0.9	0.9	-1.4	-2.9	0.29	-0.06	–	–
02A01	1	44	44	0.3	0.3	2.8	2.8	4.2	4.2	1.5	1.5	2.5	2.5	0.9	0.9	-2.5	-2.5	0.69	0.69	12	121
07A03	1	44	19	1.0	2.3	2.5	5.7	4.8	7.3	1.9	1.3	2.3	5.1	0.9	0.9	-1.5	-3.5	0.48	0.27	45	110
07A04	1	44	22	1.3	2.5	4.2	8.3	8.8	12.4	2.1	1.5	3.6	7.0	0.9	0.8	-2.9	-5.9	0.68	0.59	56	185
Total	108	4752	1664	0.8	2.1	1.3	3.6	2.9	4.9	2.2	1.4	1.1	2.8	0.8	0.8	-0.5	-1.5	0.50	0.28	–	–

(b) 2012, 27^{th} and 28^{th}, September Event

PERSIANN-CCS, spatial resolution $\approx 4 \times 4\,km^2$

Name	nº gau	Obs.	*Obs.	$\overline{qpe}$	*$\overline{qpe}$	$\overline{gau}$	*$\overline{gau}$	RMSD	*RMSD	rRMSD	*rRMSD	MAD	*MAD	rMAD	*rMAD	Bias	*Bias	R	*R	$\sum qpe$	$\sum gau$
G-No	8	216	97	3.0	6.6	4.2	9.4	11.0	16.4	2.6	1.8	4.5	9.8	1.1	1.0	-1.2	-2.8	0.32	0.13	–	–
R. Pli	6	162	92	2.5	4.4	3.8	6.6	10.0	13.2	2.6	2.0	4.3	7.5	1.1	1.1	-1.3	-2.1	0.08	-0.11	–	–
05P03	1	27	11	2.6	6.5	5.2	12.6	6.8	10.6	1.3	0.8	2.8	6.8	0.5	0.5	-2.5	-6.1	0.90	0.86	72	139
CR52	1	27	17	2.2	3.4	4.6	7.0	7.2	9.1	1.6	1.3	3.1	4.7	0.7	0.7	-2.3	-3.6	0.43	0.29	60	123
LO21	1	27	11	2.4	5.7	4.4	10.6	13.5	21.2	3.1	2.0	5.3	12.8	1.2	1.2	-2.0	-4.9	0.39	0.16	64	118
Total	107	2889	1379	2.0	4.1	2.7	5.6	7.7	11.1	2.8	2.0	3.3	6.8	1.2	1.2	-0.7	-1.5	0.18	-0.02	–	–

(c) 2016, 17-19, December Event

PERSIANN-CCS, spatial resolution $\approx 4 \times 4\,km^2$

Name	nº gau	Obs.	*Obs.	$\overline{qpe}$	*$\overline{qpe}$	$\overline{gau}$	*$\overline{gau}$	RMSD	*RMSD	rRMSD	*rRMSD	MAD	*MAD	rMAD	*rMAD	Bias	*Bias	R	*R	$\sum qpe$	$\sum gau$
Al	9	603	330	1.5	2.8	2.5	4.4	4.4	5.9	1.7	1.3	2.2	3.9	0.9	0.9	-1.0	-1.7	0.32	0.12	–	–
NE. Al	5	335	181	1.6	3.0	3.1	5.7	5.2	7.1	1.7	1.3	2.3	4.2	0.7	0.7	-1.5	-2.7	0.51	0.33	–	–
G-Re	7	469	282	1.4	2.3	2.6	4.2	3.5	4.5	1.3	1.1	2.1	3.4	0.8	0.8	-1.3	-2.0	0.41	0.19	–	–
07E01	1	67	38	1.7	2.8	2.7	4.7	6.2	8.3	2.3	1.7	2.4	4.0	0.9	0.8	-1.1	-1.9	0.14	-0.08	111	184
MU52	1	67	38	1.8	3.1	2.8	4.8	4.2	5.6	1.5	1.1	2.6	4.5	0.9	0.9	-1.0	-1.7	0.25	-0.13	119	187
P3260	1	67	42	1.7	2.7	3.1	4.8	4.4	5.5	1.4	1.1	2.5	3.8	0.8	0.8	-1.4	-2.1	0.44	0.29	114	211
Total	140	9380	4425	1.0	2.1	1.7	3.3	3.1	4.5	1.9	1.4	1.6	3.2	1.0	1.0	-0.6	-1.2	0.34	0.13	–	–

Radar, SRI product in long range mode, spatial resolution $\approx 1 \times 1\,km^2$

Name	nº gau	Obs.	*Obs.	$\overline{qpe}$	*$\overline{qpe}$	$\overline{gau}$	*$\overline{gau}$	RMSD	*RMSD	rRMSD	*rRMSD	MAD	*MAD	rMAD	*rMAD	Bias	*Bias	R	*R	$\sum qpe$	$\sum gau$
Al	11	737	417	0.8	1.2	2.4	4.1	4.2	5.6	1.8	1.4	2.1	3.4	0.9	0.8	-1.6	-2.9	0.29	0.07	–	–
NE. Al	5	335	178	1.0	1.7	3.1	5.8	5.8	8.0	1.9	1.4	2.6	4.7	0.8	0.8	-2.1	-4.1	0.42	0.21	–	–
G-Re	7	469	276	1.3	2.0	2.6	4.3	3.2	4.1	1.2	1.0	1.8	2.9	0.7	0.7	-1.3	-2.3	0.58	0.31	–	–
07E01	1	67	35	1.0	1.8	2.7	5.2	6.0	8.3	2.2	1.6	2.3	4.3	0.8	0.8	-1.8	-3.4	0.30	0.05	67	184
MU52	1	67	35	1.3	2.3	2.8	5.2	3.6	4.9	1.3	0.9	2.0	3.7	0.7	0.7	-1.5	-2.9	0.50	0.08	87	187
P142818	1	67	39	0.8	1.2	3.0	5.0	5.7	7.5	1.9	1.5	2.7	4.6	0.9	0.9	-2.2	-3.8	0.15	-0.03	53	198
Total	151	10117	4738	1.0	1.9	1.6	3.3	2.7	3.9	1.6	1.2	1.3	2.5	0.8	0.8	-0.7	-1.5	0.43	0.19	–	–

nº gau: number of raingauges, Obs.: Number of observations, $\overline{qpe}$: mean rainfall in corresponding pixels, $\overline{gau}$: mean rainfall in corresponding raingauges, RMSD: Root mean square differences, rRMSD: relative RMSD, MAD: mean absolute differences, rMAD: relative MAD, R: Pearson correlation coefficient, $\sum qpe$: Accumulated rainfall in the pixel for the whole event, $\sum gau$: Accumulated rainfall in the raingauge for the whole event. The * symbol indicates conditional statistics. S. Al: Basin located at South of rambla of El Albujón, Al: Rambla of El Albujón basin, NE. Al: Basin located at Northeast of rambla of El Albujón, G-No: Rambla of Nogalte basin, R. Pli: Pliego river basin and G-Re: Subasin of Guadalentin river where the Reguerón channel is located.

conditional RMSD values increase to 5.2 and 4.9 mm/h, respectively. The relative values of RMSD indicate that the statistic is 1.8 times the mean precipitation value of PERSIANN-CCS and 1.4 times that of radar. Both PERSIANN-CCS and radar show worse agreements with the rain gauges located in the basins most affected by the storm. The cumulative totals of the rain gauges and the pixels intersecting with them ($\sum gau$ and $\sum qpe$) show that both QPEs underestimate rainfall. The rain gauge 02A01 registered 121 mm, while the corresponding PERSIANN-CCS pixel registered only 21 mm; radar underestimations are even larger, as it only registered 12 mm. Although these data seem to be conclusive, it is important to remember the reservations that should be borne in mind when comparing a single point value with a single pixel. For the whole study area, the *bias values of PERSIANN-CCS indicate that the underestimated values compensate for the overestimated values. This is not always the case at sub-basin level. At least in one of the basins PERSIANN-CCS underestimates an average of 2.1 mm/h. This value amounts to 2.9 mm/h for the conditional bias. Both bias and *bias values are larger with radar for the whole study area, sub-basins and individual rain gauges. Correlation values, on the other hand, both conditional and non-conditional, are larger with radar in all cases.

No radar data were available for the 2012 event (Table 1 b). PERSIANN-CCS statistics shows some degree of agreement with those of the 2009 event. The *RMSD and *MAD are larger and this increase is proportional to the variation in precipitation intensity, which in the 2012 event was greater. *rRMSD and *rMAD values remain constant. In the 2012 event bias and *bias values indicate that PERSIANN-CCS as a whole underestimates precipitation and the correlation values indicate that the linear association is not strong, although it is high in the case of the 05P03 rain gauge. It appears that PERSIANN-CCS estimated approximately 50 percent of the rainfall recorded by the rain gauges.

For the 2016 event (Table 1 c) another radar (SRI) was used as QPE. The SRI takes into account the convective or stratified nature of precipitation and is assumed to be a more advanced QPE than the CAPPI product. In this event the radar was working in the long range mode, so the spatial resolution of the images was $1 \times 1\ km^2$. More rain gauges were available due to the extension of the SAIH-Segura network. In a first analysis the values of *RMSD and *MAD are similar to those of the 2009 episode. Significant changes in statistics can be seen when moving from conditional to non-conditional statistics. In the two QPEs, precipitation tends to be underestimated, the values for the whole basin being similar in both; however, if the most affected basins are taken into account, in two of them the *bias is unfavourable to radar and in the third the values are the same. With respect to the correlation of the whole area, radar shows values that are closer to those of the rain gauges, both conditional and non-conditional, but if the three basins analyzed are considered, the situation is variable. When it comes to the accumulation recorded by rain gauges, PERSIANN-CCS underestimates (111 mm versus 184 mm and 114 mm versus 211 mm), less than radar (67 mm versus 184 mm and 53 mm versus 198

Preprints (www.preprints.org) | NOT PEER-REVIEWED | Posted: 9 May 2018 doi:10.20944/preprints201805.0150.v1

Peer-reviewed version available at Remote Sens. 2018, 10, 1023; doi:10.3390/rs10071023

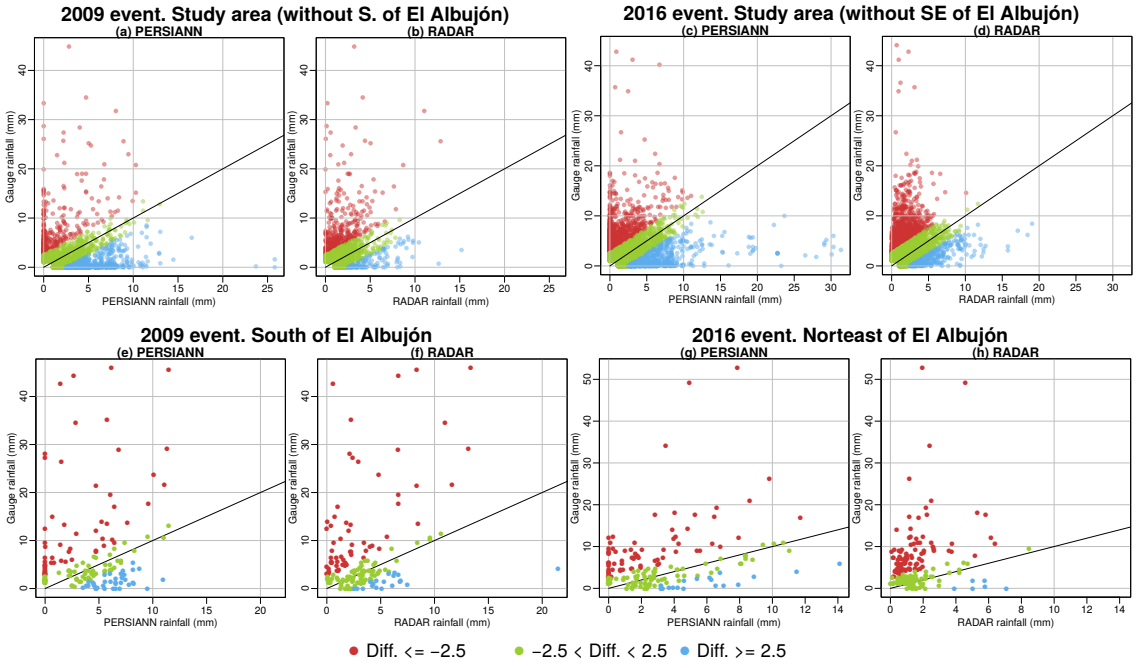

Figure 3. Scatter plots of rain gauge recorded rainfall and QPE estimations (PERSIANN-CCS and radar) during the 2009 and 2016 events.

mm). For this episode and according to the data provided by this table, it cannot be said that either QPE gives results that are more similar to the rain gauge results.

3.2. Scatter plots

Figures 3 and 4 show the scatterplots of QPEs (ordinate axis) and rain gauges (abscissa axis). The magnitude of the observed difference has been codified by colors. Only the pairs of points in which either $qpe_i \leq 1$ or $gau_i \leq 1$ are represented.

In the 2009 event, excluding the small coastal basins, the linear association between both QPEs and the rain gauges (Figures 3a and b) is weak. In the case of PERSIANN-CCS there are many values

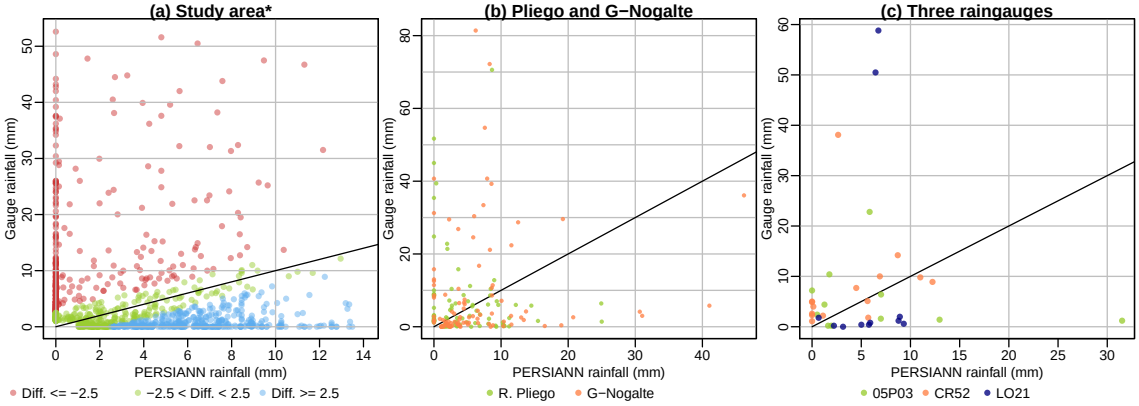

Figure 4. Scatter plots of rain gauge recorded rainfall and QPE estimations (PERSIANN-CCS and radar) during the 2012 event.

above the line $y = x$. Of note is the fact that very high rainfall values recorded by the rain gauges are recorded as just over 5-10 mm/h in PERSIANN-CCS, and that considerably high rainfall values are estimated as zero by this QPE. The radar might be expected to produce better results, but this is not the case, as there are also many points above the line $y = x$. The points with $|diff_i| < 2.5$ (green dots) in PERSIANN-CCS account for 51.8 percent, while on radar they represent 68.7 percent of the points. The most noteworthy difference between radar and PERSIANN-CCS corresponds to the points representing an overestimation of more than 2.5 mm/h (blue points). In PERSIANN-CCS these cases represent 29.6 percent while on radar they represent 7.7 percent. If we focus the analysis on the coastal basins (where the greatest accumulations of precipitation were reached), the absence of a linear correlation is also evident between the two estimates for the two QPEs. There is a significant number of cases where $diff_i$ is greater than 2.5 mm/h and very high intensities (above 40 mm/h) are estimated by both QPEs as 2, 3, 5 or 11 mm/h. The maximum value that PERSIANN-CCS and radar estimate acceptably well is around 10-11 mm/h (higher value reached on the X axis by a green dot). The number of points with significant overestimation of precipitation (blue points) is higher in PERSIANN-CCS, although the maximum in this sense is obtained by radar, which, on one occasion, estimated 22 mm/h when the rain gauge collected about 5 mm/h.

In the 2016 event the results are similar. Points with $|diff_i| < 2.5$ in PERSIANN-CCS represent 52 percent and 67.1 percent on radar. Again, the percentage of $diff_i > 2.5$ is much higher in PERSIANN-CCS (15.7 percent) than in radar (6.7 percent). PERSIANN-CCS presents several cases of overestimation (blue dots), and there are at least 8 dots where it estimated around 30 mm/h while the rain collected around 5 mm/h. This is much less marked on radar. In the coastal basins, the patterns of 2009 episode are repeated. In this case, the highest acceptably well estimated value by PERSIANN-CCS is around 11 mm/h, whereas on radar it is 8.5 mm/h.

The scatter plots for the 2012 event (Figure 4) are different because no radar data were available for comparison. In addition, the storm was much shorter but more intense than in 2016 and 2009, which is why there are fewer points on the scatter plot in Figure 4 a. Especially striking are the points where the rain gauges register very strong intensities, up to 55 mm/h for seven hours but PERSIANN-CCS registers zero. At 31.2 percent of the points $diff_i < -2.5\ mm/h$. If we focus on the two basins that received the greatest accumulations (Pliego river and Guadalentín - Nogalte), it is seen that the highest hourly intensities of the three storms (more than 80 mm/h) are estimated by PERSIANN-CCS at around 8 mm/h, while values higher than the 70 mm/h are estimated at around 9 mm/h. By contrast, PERSIANN-CCS estimates of more than 30 mm/h are recorded as 8 mm/h by rain gauges.

Preprints (www.preprints.org) | NOT PEER-REVIEWED | Posted: 9 May 2018 doi:10.20944/preprints201805.0150.v1

Peer-reviewed version available at Remote Sens. 2018, 10, 1023; doi:10.3390/rs10071023

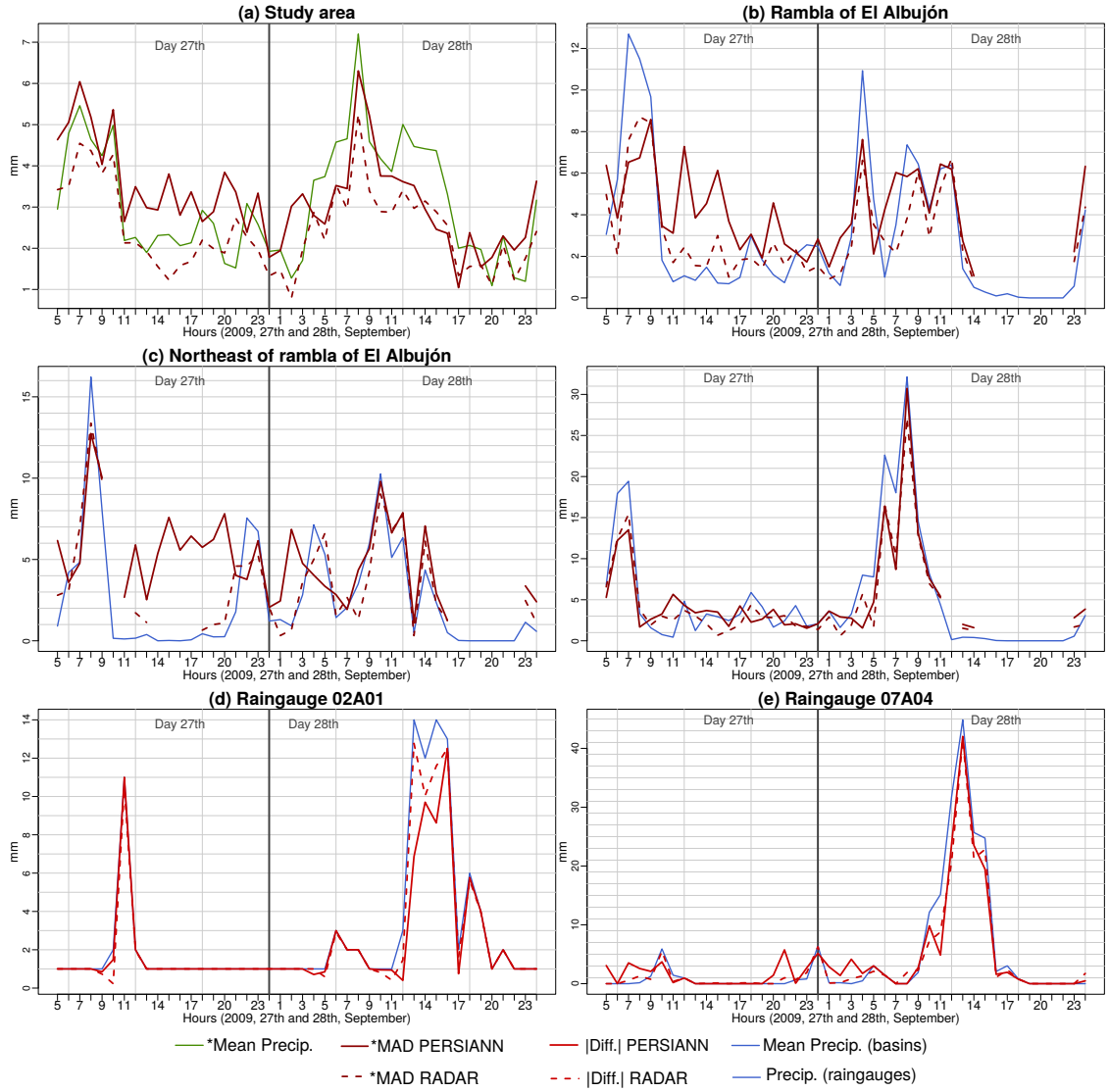

Figure 5. Temporal variation of several statisticians in different spatial areas of the study area (PERSIANN-CCs and radar) during the 2009 event.

3.3. Hourly monitoring of storm

The analysis of the temporal evolution of the intensities and of the agreement measures between the two estimates give an indication of the virulence of the storm as well as the possible hydrological response of the basin. This analysis is also important to validate precipitation products as it allows us to assess whether the QPE analyzed, in the absence of other sources of information, correctly estimates the evolution of the storm or the quantities precipitated in small basins prone to flash floods.

In real-time flood monitoring and population warning, it is more interesting to know the agreement between the two sources of information when the highest intensities are reached. Overestimation problems are also important, but underestimation problems are critical in emergency situations.

Preprints (www.preprints.org) | NOT PEER-REVIEWED | Posted: 9 May 2018 doi:10.20944/preprints201805.0150.v1

Peer-reviewed version available at Remote Sens. 2018, 10, 1023; doi:10.3390/rs10071023

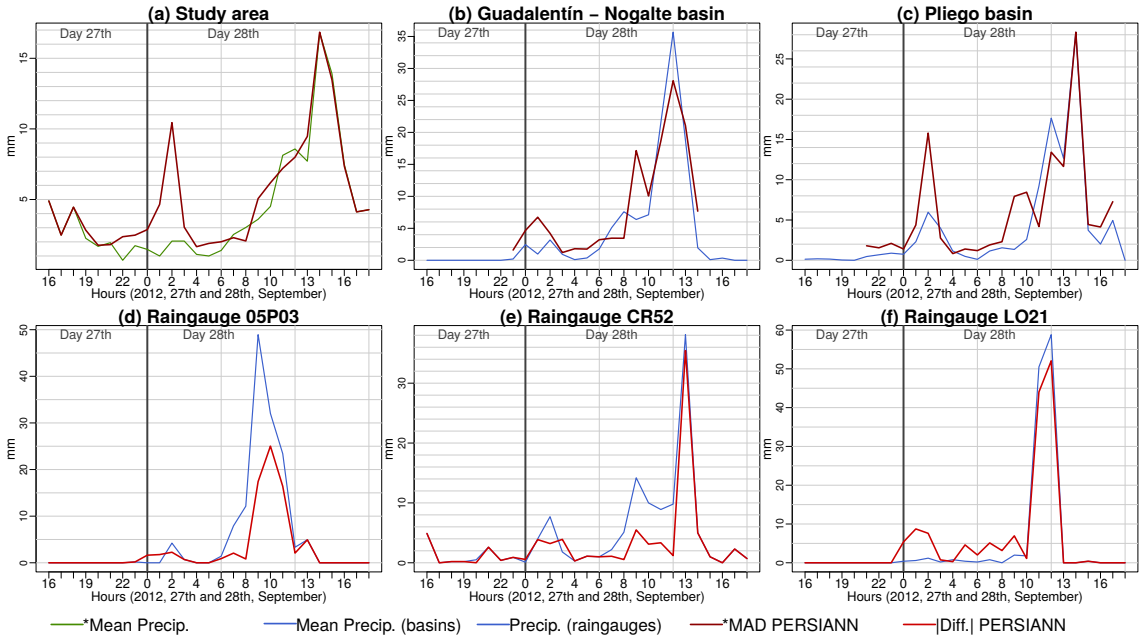

Figure 6. Temporal variation of several statisticians in different spatial areas of the study area (PERSIANN-CCS) during the 2012 event.

Figure 5 shows the evolution of the mean conditional precipitation according to rain gauges and the conditional MAD for the whole study area and for the three coastal basins, and the precipitation according to rain gauges and the difference in precipitation in absolute values for two rain gauges.

In the study area, both PERSIANN-CCS and radar *MAD values are very similar to $\overline{gau}$ when this value is high (Figure 5 a). The *MAD of radar tends to be low when the $\overline{gau}$ is low, while this is not the case with PERSIANN-CCS. If we focus on the rain gauges of the Albujón basin we see that the *MAD is proportional to the intensity of the precipitation and the peaks of *MAD in both PERSIANN-CCS and radar coincide with the two peaks of $\overline{gau}$. In some time intervals the PERSIANN-CCS *MAD and radar lines disappear because there were not enough valid data to calculate the statistics. This happens when neither rain gauges nor QPEs recorded rainfall. For the other two basins and the two rain gauges analysed, the results are similar. Both PERSIANN-CCS and radar have very high *MAD for the magnitude of $\overline{gau}$ and very high $|Diff|$ for precipitation amount.

Figure 6 shows the results for the 2012 event. Conditional *MADs coincides with average precipitation at peak precipitation levels and again there is overestimation when average precipitation is low.

The results of the 2016 event are shown in Figure 7. In the study area, the temporal evolution of the *MAD indicates that this statistic, as in previous events, is closely related to the precipitation recorded by the rain gauges, although PERSIANN-CCS overestimates precipitation when it was low. The *MADs of PERSIANN-CCS shows very erratic estimations, with strong ups and downs in very

Preprints (www.preprints.org) | NOT PEER-REVIEWED | Posted: 9 May 2018 doi:10.20944/preprints201805.0150.v1

Peer-reviewed version available at Remote Sens. 2018, 10, 1023; doi:10.3390/rs10071023

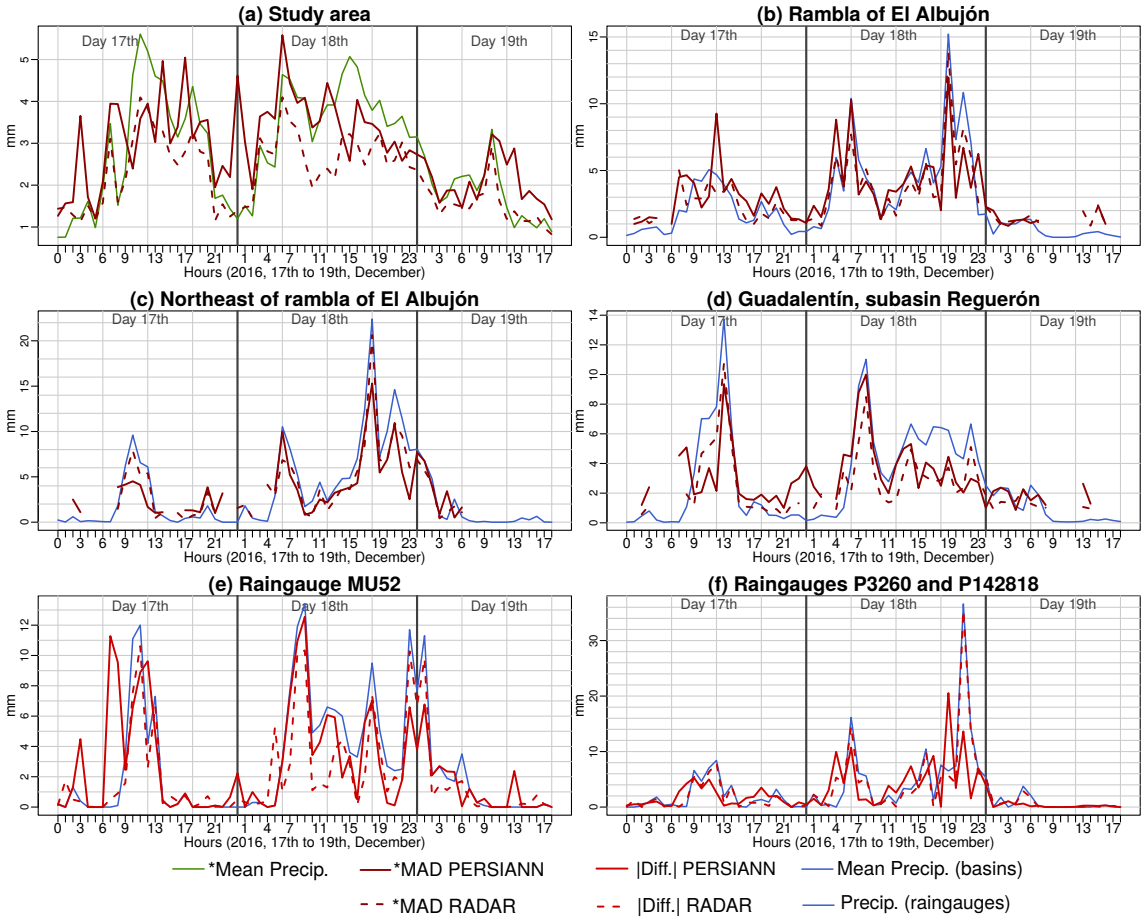

Figure 7. Temporal variation of several statisticians in different spatial areas of the study area (PERSIANN-CCs and radar) during the 2016 event.

short periods of time. In this sense, radar *MADs are much more constant and correlated for both high and low mean precipitation values. Radar patterns are more accurate than those of PERSIANN-CCS. The results for the three basins most affected by the storm (Figure 7) point to a much more similar behaviour between the two QPEs. Again, average precipitation peaks reflect peaks in *MAD in the two QPEs, although the *MAD values of PERSIANN-CCS are usually higher. Similar conclusions can be drawn from the analysis of the two rain gauges, except for some precipitation peaks when radar is the QPE which differs most from the values recorded by the rain gauges.

The statistics of the three events and the three analyzed scales show a similar pattern. The highest values correspond to the highest precipitation intensities recorded by the rain gauges. In some cases the differences are larger in PERSIANN-CCS and in others in radar, although the former are more frequent. In addition, PERSIANN-CCS overestimates rainfall during stormy events when rain gauges records were small.

Preprints (www.preprints.org) | NOT PEER-REVIEWED | Posted: 9 May 2018 doi:10.20944/preprints201805.0150.v1

Peer-reviewed version available at Remote Sens. 2018, 10, 1023; doi:10.3390/rs10071023

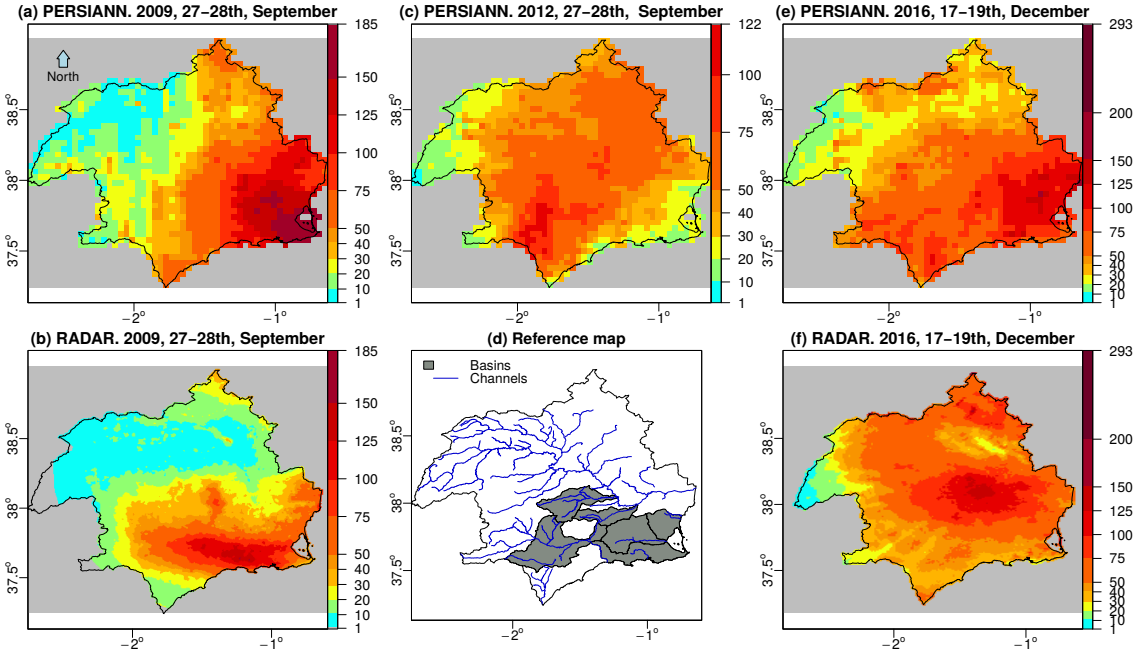

Figure 8. Total precipitation accumulations of the three events in *mm*. WGS projection (EPSG code 4326). (**a**) and (**b**) from 0500 UTC Sep 27 to 0100 UTC 30 Sep 2009. (**c**) from 1600 UTC 27 Sep to 1900 UTC 28 Sep 2012. (**e**) and (**f**) from 0000 UTC 17 Dec to 1900 UTC 19 Dec 2016.

3.4. Side-by-side comparison of accumulated precipitation

In order to correctly validate QPEs, the map of precipitation accumulations of the whole event was compared with the map of the differences observed (Figures 8 and 9) for the two QPE and the three events analyzed. When data from both QPEs (2009 and 2016 events) were available, the legends are common in order to facilitate comparison. Each map was generated with the native resolution of the QPE, which is evident from the appearance of the maps, especially in the case of the 2009 event, when the radar worked in short-range mode with a spatial resolution of $500 \times 500\ m^2$, but does not covere the entire study area as its range is only a 120 km radius. To interpolate the rain gauge results (Figure 9) we used inverse distance weighting and ordinary kriging with automatic fitting procedures using the R geostatistical library *gstat* [35]. Leave-One-Out Cross-Validation was used to select the better of both interpolation methods.

The 2009 event shows an east-west rainfall gradient according to PERSIANN-CCS, with the highest values in the east. The maximum value of this QPE is 184 mm and the average value is 50 mm. The radar estimate for the 2009 episode, on the other hand, seems to be distributed in horizontal bands, with the highest values concentrated at the latitude of the coastline of the Region of Murcia descending towards the north and towards the south. The maximum radar accumulation value in this episode is 154 mm and the average is 30.7 mm, both much lower than the values provided by PERSIANN-CCS. With regard to the interpolation of differences (Figure 9 a and b), the PERSIANN-CCS map shows

Preprints (www.preprints.org) | NOT PEER-REVIEWED | Posted: 9 May 2018 doi:10.20944/preprints201805.0150.v1

Peer-reviewed version available at Remote Sens. 2018, 10, 1023; doi:10.3390/rs10071023

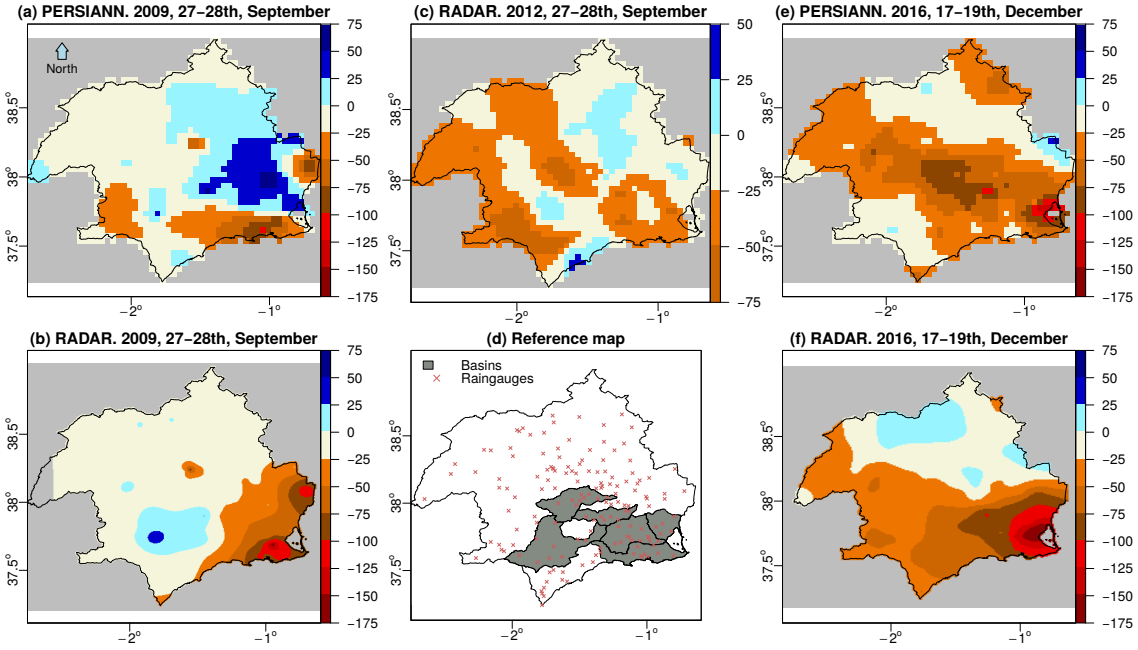

Figure 9. Interpolation by Ordinary Kriging of the total accumulation differences (PERSIANN-CCS minus rain gauge) in each event in *mm*. WGS84 projection (EPSG code 4326). (**a**) and (**b**) from 0500 UTC 27 Sep to 0100 UTC 30 Sep 2009. (**c**) from 1600 UTC 27 Sep to 1900 UTC 28 Sep 2012. (**e**) and (**f**) from 0000 UTC 17 Dec to 1900 UTC 19 Dec 2016.

both overestimation in the northern part of the Mar Menor lagoon, the northern part of the Campo de Cartagena and the horticultural area around Murcia, and underestimation, although moderate, along the southern coast. The mean of the absolute values of the map is 17.7 mm, while the same statistic on the radar map is 19.4 mm. With respect to the maximums, the PERSIANN-CCS is 104.5 mm and the radar is 169.2 mm. The map of interpolated radar differences (Figure 9 b) shows very strong underestimations near Cartagena and the mouth of the Segura river, while these values tend to fall in a north-westerly direction. There is a small nucleus of overestimation around the city of Lorca.

With respect to the 2012 episode (Figure 8 c), the largest accumulations estimated by PERSIANN-CCS are around the Nogalte and Guadalentín basins, where the largest accumulations actually occurred during this storm. The estimated accumulation values tend to fall towards the northwest and southeast. The interpolation of the differences identifies the areas where PERSIANN-CCS strongly underestimates the greatest rainfall accumulations recorded by the rain gauges. Only in a few pixels on the southern coast of the Region of Murcia rainfall is overestimated by PERSIANN-CCS.

Figures 8 e and f show the precipitation accumulations of PERSIANN-CCS and radar for the 2016 event. Apart from the different spatial resolutions, both are similar except that PERSIANN-CCS places the greatest accumulations near the SE coast and radar places them in the centre of the study area.

Preprints (www.preprints.org) | NOT PEER-REVIEWED | Posted: 9 May 2018 doi:10.20944/preprints201805.0150.v1

Peer-reviewed version available at Remote Sens. 2018, 10, 1023; doi:10.3390/rs10071023

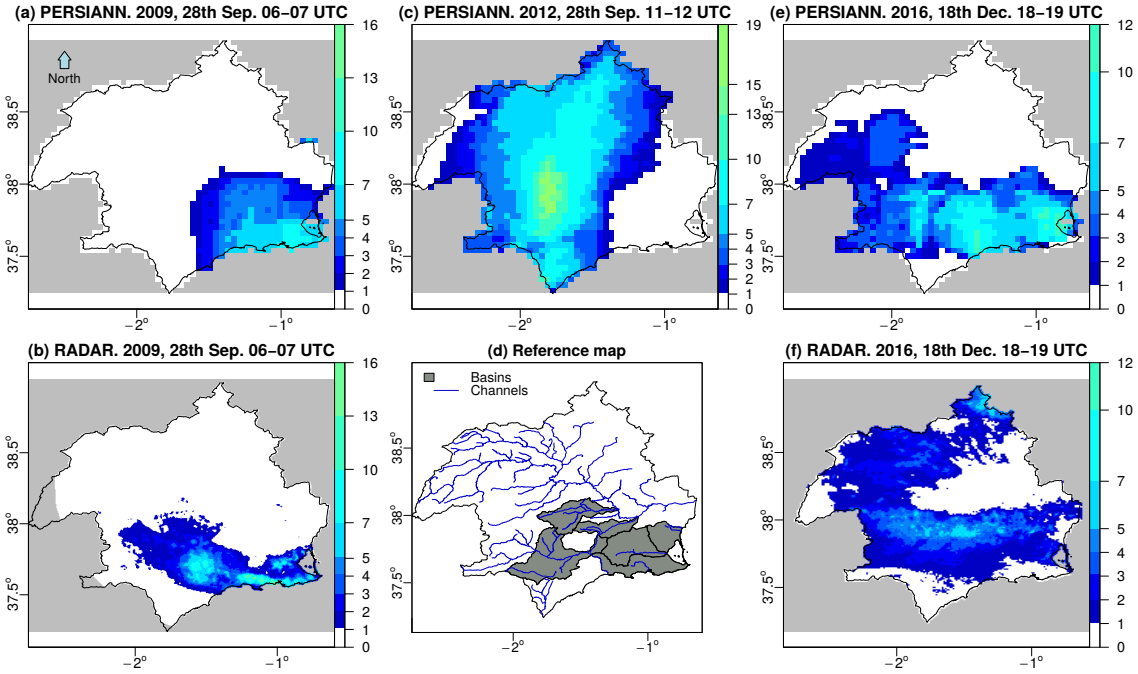

Figure 10. Maximum hourly accumulations of precipitation according to rain gauges of the three events in *mm*. WGS projection (EPSG code 4326).

With regard to the differences, Figures 9 e and f show that the greatest differences are found in the SE coast, although, due to its size, these differences are greater in the case of radar.

3.5. Side-by-side comparision of maximum hourly rainfall intensity

It is also interesting to study the differences between QPE and rain gauges estimations in the time intervals with higher precipitation intensities. For each event, the highest intensity time lapse in each rain gauge was identified in the hietographs (Figures 13 a and d and 14 a). Figure 10 presents the hourly precipitation estimates for the two QPEs and Figure 11 presents the interpolations of the differences between the QPE and the rain gauges, using the same method as for the total accumulation differences.

With respect to the maximum hourly precipitation in the 2009 event (Figure 10 a and b), there are important differences between the two QPEs. During the hour of maximum intensity, precipitation has only affected one sector of the study area, while the identification of this area is different in the two QPEs. The maximum precipitation is identified by PERSIANN-CCS between the city of Cartagena and Cabo de Palos, while radar identifies two nuclei of heavy precipitation, one north of Cabo Tiñoso and the other in the Guadalentín valley, near the city of Lorca. Both QPEs underestimate the rainfall recorded by rain gauges in the same area, west of the city of Cartagena.

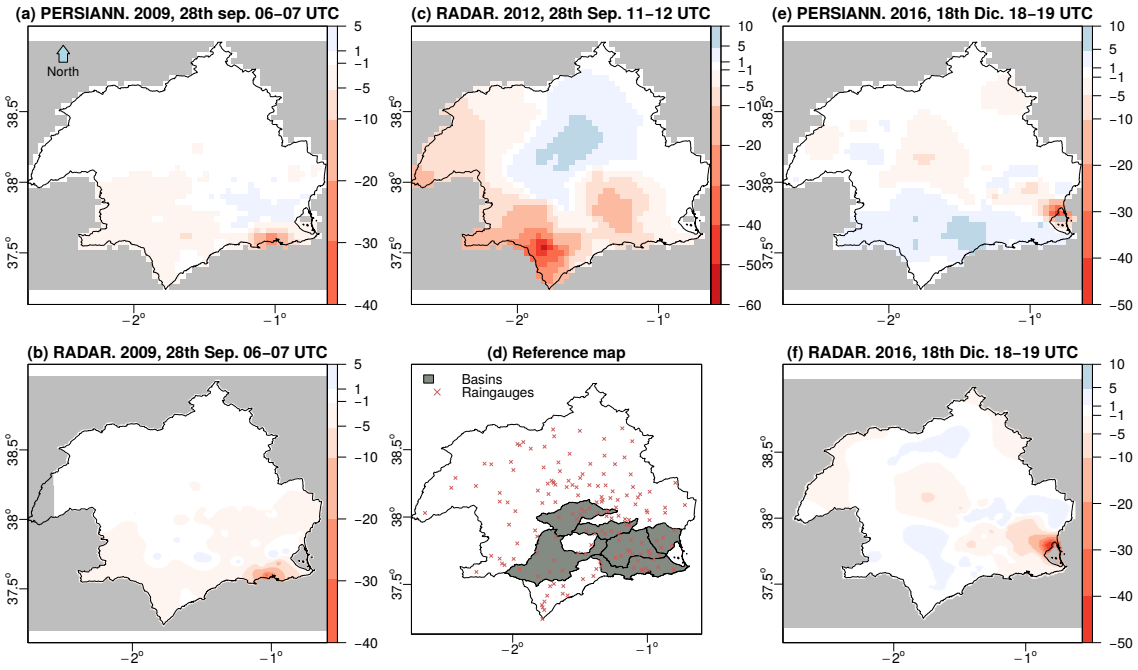

Figure 11. Interpolation by IDW (**a**) and Ordinary Kriging (**b** to **f**) of the differences (QPE minus pluviometer) of maximum hourly accumulation in each event in mm/h. WGS84 projection (EPSG code 4326).

With respect to the 2012 event (Figure 10 c) PERSIANN-CCS places the maximum intensities at a different place to the rain gauge records, and underestimates rainfall (by between 40 and 60 mm/h) in the Guadalentín and Nogalte basins.

With respect to the 2016 event (Figure 10 e and f), the spatial distribution of the two QPEs shows some similarities, at least in the precipitation pattern. PERSIANN-CCS estimates higher precipitation values (third quartile equals 3.7 mm and maximum value equals 11.7) than radar (2.3 mm and 7.7 mm, respectively). The map of the interpolated differences indicates that both QPEs underestimate rainfall, especially in the areas where the rain gauges have recorded the highest intensities. The bias of the PERSIANN-CCS differences is -0.11 mm while in radar the bias is -0.98 mm. The minimum value with PERSIANN-CCS is -41.7 mm and with radar -50.7 mm. Considering the higher spatial resolution of radar compared with PERSIANN-CCS, it is of note that, for this particular time in the storm, PERSIANN-CCS produces better results than radar.

3.6. Spatial statistics

Using the radar precipitation as baseline, spatial statistics were calculated for PERSIANN-CCS and radar. Figure 12 highlights these spatial relationships. The upscaling procedure applied for radar consisted in transferring values from the high-resolution raster cells to each one of the 0.04º grid cells using bilinear interpolation as implemented of the `resample` function of the raster R package [36]. Considering that the resampling was applied at an hourly timescale in which precipitation is assumed

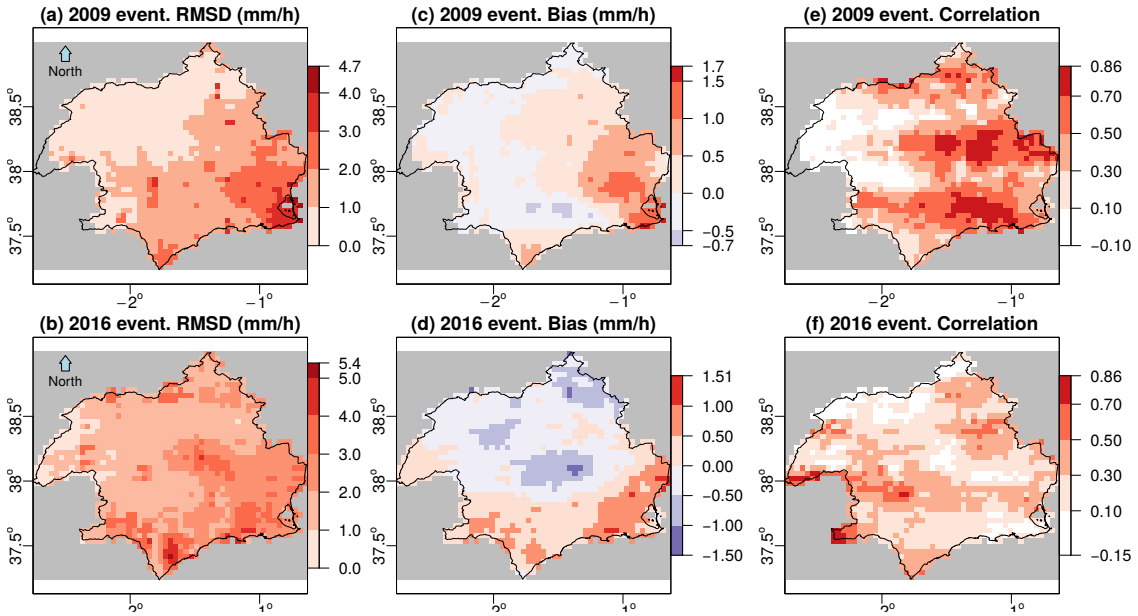

Figure 12. Comparision statistics between PERSIANN-CCS and radar hourly precipitation. WGS84 projection (EPSG code 4326). (**a**), (**c**) and (**d**) from 0500 UTC 27 Sep to 0100 UTC 30 Sep 2009. (**a**), (**c**) and (**d**) from 0000 UTC 17 Dec to 1900 UTC 19 Dec 2016.

to be a smoothly varying variable within each 0.04° grid cell, we consider the bilinear interpolation to be a suitable technique with no or low impact on our results. The same procedure was applied by Zambrano-Bigiarini *et al.* (2017) [12] on a daily scale. In the 2009 event, the highest RMSD values appear in the coast, where the maximum rainfall values were recorded. RMSD decreases in a SE-NW direction. 83 % of the study area shows RMSD equal to or smaller than 2 mm/h, and only 5 pixels shows a value higher than 4 mm/h, so the agreement between both QPEs is high. RMSD values for the 2016 event are not homogeneously distributed and the differences values are higher near the coast, although not exactly where rainfall was more intense. In this case, the RMSD values below 2 mm/h decrease to 56 percent, while 19 pixels has an RMSD equal to or greater than 4. The area covered by very low RMSD values of less than 1 mm/h is much smaller than in the 2009 episode.

Figure 12 c and d shows the bias of each pixel. In the 2009 event, the pixels with a bias less than 0 (assuming the radar data as the baseline) is 41%, which is much lower than for the 2016 event. As regards the correlation (Figure 12 e and f), high correlation values are much more frequent in the 2009 event. Both QPEs are similar in the 2009 event and less so in the 2016 event.

3.7. Hyetographs

Finally, the precipitation estimates of three pluviometers and the corresponding pixels of the two QPEs were compared for each event, three rain gauges were selected: the ones with the highest hourly rainfall intensity, the highest rainfall accumulation, and the rainfall accumulation closest to the average cumulative precipitation of all the rain gauges.

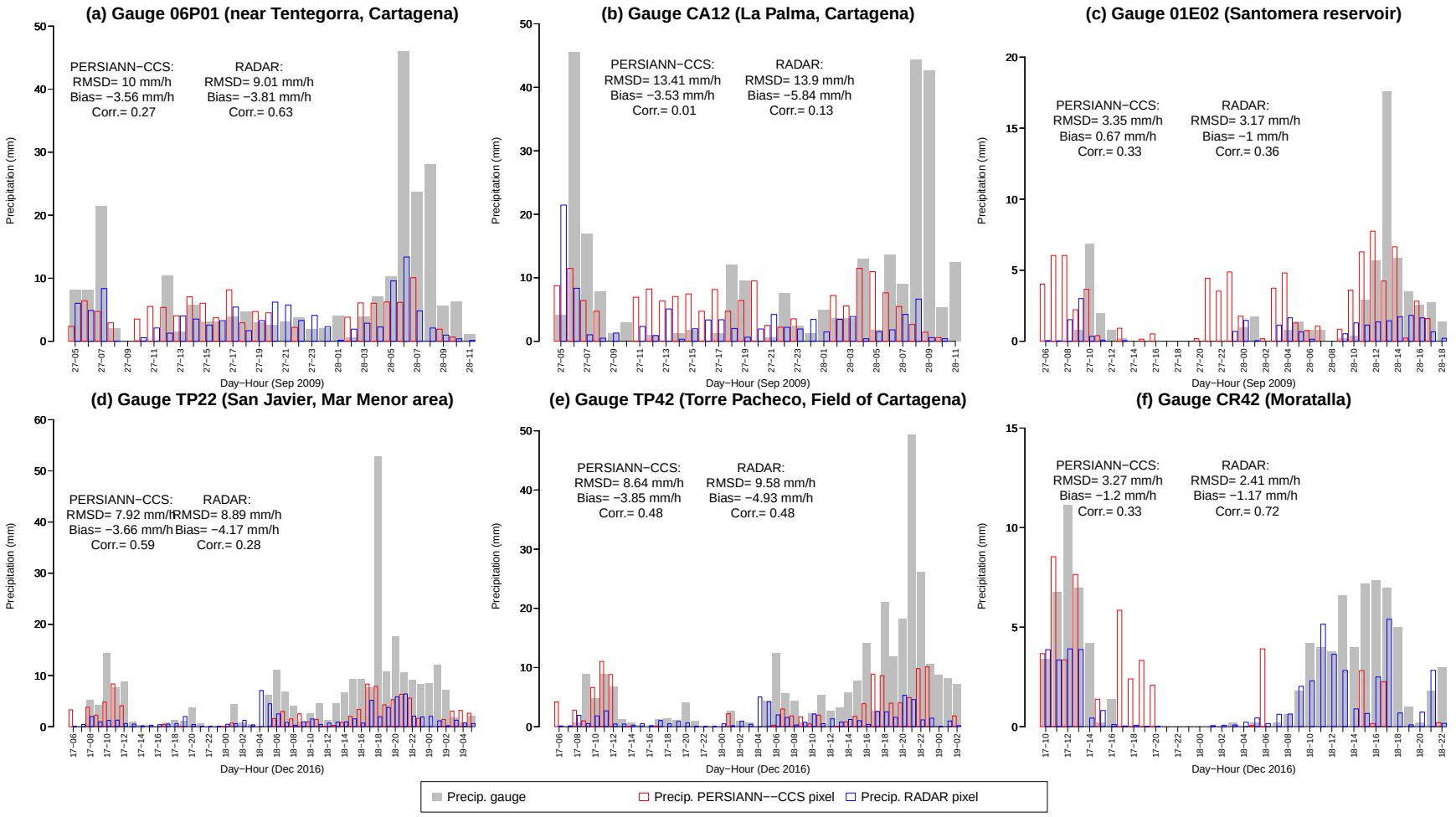

Figure 13. Hyetographs and associated statistics of PERSIANN-CCS, radar and the corresponding rain gauges of SIAM or SAIH-Segura. (**a**), (**b**) and (**c**), 2009 event. (**d**), (**e**) and (**f**), 2016 event .

Preprints (www.preprints.org) | NOT PEER-REVIEWED | Posted: 9 May 2018 doi:10.20944/preprints201805.0150.v1

Peer-reviewed version available at Remote Sens. 2018, 10, 1023; doi:10.3390/rs10071023

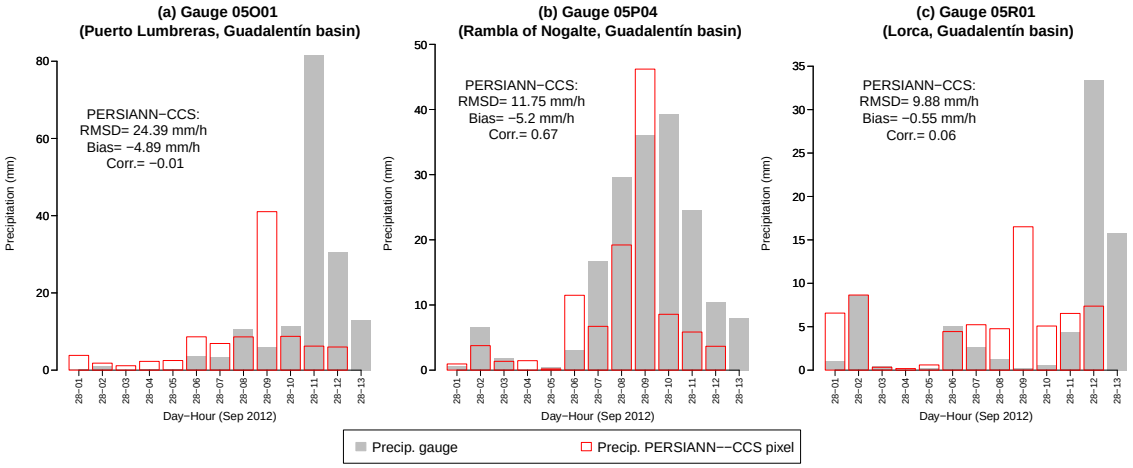

Figure 14. Hyetographs and associated statistics of PERSIANN-CCS and the corresponding rain gauges of SAIH-Segura.

Starting with the precipitation observed in the 2009 hietographs, it is clear that both QPEs significantly underestimate rainfall. In the case of the rain gauge with the highest hourly intensity, both QPEs correctly detect the presence of precipitation, but not its quantity. In the hour with the highest intensity, radar is more accurate, in the hour with the second highest intensity, PERSIANN-CCS does not detect precipitation and radar shows minimum intensity. In the case of the highest accumulation rain gauge (Figure 13 b), the highest precipitation intensities are not captured by any of the QPEs. The same can be said for the most representative total accumulation rain gauge. These results are similar for the 2012 and 2016 events.

4. Discussion and conclusion

A comparison of two QPEs with two rain gauge networks has been carried out for the most severe rainfall events in the south-east of the Iberian Peninsula in the last decade. These events had a very high return period, close to 500 years. The objective was to know if either of the QPEs could be of use in monitoring such events. The results for the three events are similar: neither PERSIANN-CCS nor radar (both without empirical calibration from rain gauges) are acceptable QPEs for real-time monitoring. The larger the rainfall intensity, the greater the disagreement of the two QPEs with the rain gauges. When aggregated data (Table 1) are used, the relative agreement statistics rMSD and *rMSD, are higher than the mean precipitation and, in the case of rMAD and *rMAD, they are close to the average precipitation. When disaggregated data are analysed (the differences between a particular rain gauge and the pixel with which it intersects spatially), the differences between the two estimates are found very high. The underestimation is very high when rainfall recorded by rain gauges is also very high. The highest precipitation correctly identified by the two QPEs ($\pm 2.5\ mm/h$) are around 10-12 mm/h, both in PERSIANN-CCS and radar. This is a fairly low value, given that the maximum

Peer-reviewed version available at Remote Sens. 2018, 10, 1023; doi:10.3390/rs10071023

intensities reached in the three storms were four times this value in several cases (Figure 13 and 14), and in one case it reached 80 mm/h (Figure 14 b). Neither of the two QPEs adequately represent the time point precipitation recorded by the the rain gauges. The total cumulations of the two QPEs also show significant differences. In the 2009 event, the radar underestimation is greater than that of PERSIANN-CCS, but the latter significantly overestimates, which is not the case with radar. In the 2016 event, the areas with larger underestimations coincide partially in the two QPEs, being more concentrated and of greater magnitude in radar. It does not seem, therefore, that radar is more accurate than PERSIANN-CCS, despite its larger spatial resolution and its commonly higher effectiveness.

The results of this work agree with those of several previous contributions. On a daily scale, Burcea *et al*. (2012) [34] also found that meteorological radar underestimated rainfall recorded by rain gauges. Changing the time scale from daily to ten minutes, similar results have also been documented [37].

Several studies have documented differences in satellite-based QPE estimations when precipitation intensities are high. On a daily scale, but for a larger spatial scope, such as Chile, Zambrano-Bigiarini *et al*. (2017) [12] pointed out that PERSIANN-CCS and other satellite-based QPEs were able to correctly identify the occurence of no-rain events, but had low accuracy when classifying precipitation intensities during rainy days. Similar patterns have been identified in other mountain areas using the TRMM Multi-Satellite Precipitation Analysis (TMPA) 3B42b6 [38]. In Europe, other satellite-based QPEs have been evaluated, such as the CMORPH (Climate Center Morphing technique) of NOAA, with a spatial resolution of $8 \times 8\ km^2$ and a temporal resolution of 30 minutes [39]. These authors also highlight that this QPE underestimates rainfall when analysing heavy precipitation events. Nikolopoulos *et al*. (2013) [6] reported similar results for TRMM TMPA, CMORP and PERSIANN-CCS, pointing to the problems of underestimation of flash-floods if such products are used as input for hydrological modelling in mountainous areas. Chen *et al*. (2013) [13] compared four satellite-based QPEs, including PERSIANN-CCS, and radar, for an extreme event, the Moratok typhoon over Taiwan. Their results with PERSIANN-CCS are very similar to those presented in this paper.

Although our results are based on only three events, and do not provide statistical significance, they represent an example of satellite-based and ground-based QPE accuracies in a Mediterranean basin for three extreme storm events that caused major floods, and point to the severe underestimation shown by both products in all the events.

This work is based on a network of rain gauges that are not randomly or regularly distributed in the territory. Due to the specific purposes of the two rain gauges networks, irrigated crop areas, valley bottoms, coastal plains and places where there are relevant hydraulic infrastructures for flood management or water accumulation, mainly reservoirs, are over-represented. On the other hand, forest

or scrub areas, the upper part of the basin and the mountain peaks are under-represented (Figure 1). It is not clear the extent to which this over-representation can influence the bias of the statistics used in the research, and we suggest that this is an interesting topic to be tackled with data from other more randomly located rain gauge networks.

According to the results obtained in this work and in agreement with the literature, all these precipitation products still present serious problems when it comes to quantitatively estimating rainfall during very heavy precipitation events. Both PERSIANN-CCS and other satellite-based QPEs present the common problem of underestimating high precipitation intensities. However, it should be noted that due to its close to global coverage, its high spatial resolution, its high temporal resolution and its short lag time, this satellite-based QPE presents very good characteristics for a local calibration of an empirical type based on a network of rain gauges located in the field and providing data in real time. In case of rain gauge failures, the applicability and availability of precipitation data obtained from satellite sources, such as PERSIANN-CCS, could be of value since the methods they use to collect information are independent of local conditions.

The two analysed QPEs do not reproduce the spatio-temporal variability of heavy rainfall events. However, it is possible that they could serve as predictors when interpolating rainfall on sub-daily scales using machine learning regression algorithms.

Acknowledgments: This work is the result of a postdoctoral contract funded by Saavedra Fajardo programme (Ref. 20023/SF/16) of the Consejería de Educación y Universidades of CARM (Autonomous Community of Murcia Region), by the Fundación Séneca-Agencia de Ciencia y Tecnología de la Región de Murcia. The support and availability of information from the Center for Hydrometeorology and Remote Sensing of University of California-Irvine (USA), from the Segura Basin Hydrological Confederation (CHS) and from Instituto Murciano de Investigación y Desarrollo Agrario y Alimentario (IMIDA) of CARM are also acknowledged. Source radar data were provided by the Spanish Meteorological Agency (AEMET) of the Spanish Ministry of Farming and Fishing, Fooding and Environment. The authors thank Luis Bañón Peregrín, Juan Manzano Cano and José Miguel Gutiérrez (AEMET) for assistance in understanding the radar-rainfall data products available.

Author Contributions: The three authors contributed equally to this work.

Conflicts of Interest: The authors declare no conflict of interest.

References

1. Hong, Y.; Hsu, K.L.; Sorooshian, S.; Gao, X. Precipitation Estimation from Remotely Sensed Imagery Using an Artificial Neural Network Cloud Classification System. *Journal of Applied Meteorology* **2004**, *43*, 1834–1852.
2. Sun, Q.; Miao, C.; Duan, Q.; Sorooshian, S.; Hsu, K.L. A Review of Global Precipitation Data Sets: Data Sources, Estimation, and Intercomparisons. *Reviews of Geophysics* **2018**, *56*.
3. Woldemeskel, F.M.; Sivakumar, B.; Sharma, A. Merging gauge and satellite rainfall with specification of associated uncertainty across Australia. *Journal of Hydrology* **2013**, *499*, 167–176.
4. Sorooshian, S.; Nguyen, P.; Sellars, S.; Braithwaite, D.; AghaKouchak, A.; Hsu, K., Extreme Natural Hazards, Disaster Risks and Societal Implications; Cambridge University Press, 2014; chapter Satellite-based remote sensing estimation of precipitation for early warning systems, pp. 99–112.

5. Bendix, J.; Fries, A.; Zárate, J.; Trachte, K.; Rollenbeck, R.; Pucha-Cofrep, F.; Paladines, R.; Palacios, I.; Orellana, J.; Oñate Valdivieso, F.; Naranjo, C.; Mendoza, L.; Mejia, D.; Guallpa, M.; Gordillo, F.; Gonzalez-Jaramillo, V.; Dobbermann, M.; Célleri, R.; Carrillo, C.; Araque, A.; Achilles, S. RadarNet-Sur First Weather Radar Network in Tropical High Mountains. *Bulletin of the American Meteorological Society* **2017**, *98*, 1235–1254.
6. Nikolopoulos, E.I.; Anagnostou, E.N.; Borga, M. Using High-Resolution Satellite Rainfall Products to Simulate a Major Flash Flood Event in Northern Italy. *Journal of Hydrometeorology* **2013**, *14*, 171–185.
7. Miao, C.; Ashouri, H.; Hsu, K.L.; Sorooshian, S.; Duan, Q. Evaluation of the PERSIANN-CDR Daily Rainfall Estimates in Capturing the Behavior of Extreme Precipitation Events over China. *Journal of Hydrometeorology* **2015**, *16*, 1387–1396.
8. Hong, Y.; Gochis, D.; Cheng, J.t.; Hsu, K.l.; Sorooshian, S. Evaluation of PERSIANN-CCS Rainfall Measurement Using the NAME Event Rain Gauge Network. *Journal of Hydrometeorology* **2007**, *8*, 469–482.
9. Schiemann, R.; Erdin, R.; Willi, M.; Frei, C.; Berenguer, M.; Sempere-Torres, D. Geostatistical radar-raingauge combination with nonparametric correlograms: methodological considerations and application in Switzerland. *Hydrology and Earth System Sciences* **2011**, *15*, 1515–1536.
10. Michaud, J.D.; Sorooshian, S. Effect of rainfall-sampling errors on simulations of desert flash floods. *Water Resources Research* **1994**, *30*, 2765–2775.
11. Ballari, D.; Castro, E.; Campozano, L. Validation of Satellite Precipitation (TRMM 3B43) in Ecuadorian Coastal Plains, Andean Higlands and Amazonian Rainforest. The International Archives of the Photogrammetry, Remote Sensing and Spatial Information Sciences; Copernicus GmbH: Prague, Czech Republic, 2016; Vol. XLI-B8, pp. 305–311.
12. Zambrano-Bigiarini, M.; Nauditt, A.; Birkel, C.; Verbist, K.; Ribbe, L. Temporal and spatial evaluation of satellite-based rainfall estimates across the complex topographical and climatic gradients of Chile. *Hydrology and Earth System Sciences* **2017**, *21*, 1295–1320.
13. Chen, S.; Hong, Y.; Cao, Q.; Kirstetter, P.E.; Gourley, J.J.; Qi, Y.; Zhang, J.; Howard, K.; Hu, J.; Wang, J. Performance evaluation of radar and satellite rainfalls for Typhoon Morakot over Taiwan: Are remote-sensing products ready for gauge denial scenario of extreme events? *Journal of Hydrology* **2013**, *506*, 4–13.
14. Barredo, J.I. Major flood disasters in Europe: 1950-2005. *Natural Hazards* **2007**, *42*, 125–148.
15. López-Martínez, F.; Gil-Guirado, S.; Pérez-Morales, A. Who can you trust? Implications of institutional vulnerability in flood exposure along the Spanish Mediterranean coast. *Environmental Science and Policy* **2017**, *76*, 29–39.
16. Serrano-Notivoli, R.; Martín-Vide, J.; Saz, M.A.; Longares, L.A.; Beguería, S.; Sarricolea, P.; Meseguer-Ruiz, O.; de Luis, M. Spatio-temporal variability of daily precipitation concentration in Spain based on a high-resolution gridded data set. *International Journal of Climatology* **2017**.
17. AghaKouchak, A.; Behrangi, A.; Sorooshian, S.; Hsu, K.; .; Amitai, E. Evaluation of satellite-retrieved extreme precipitation rates across the central United States. *Journal of Geophysical Research* **2015**, *116*.
18. Pellicer-Martínez, F.; Martínez-Paz, J.M. Probabilistic evaluation of the water footprint of a river basin: Accounting method and case study in the Segura River Basin, Spain. *Science of the Total Environment* **2018**, *627*, 28–38.
19. Gomariz-Castillo, F.; Alonso-Sarría, F.; Cabezas-Calvo-Rubio, F. Calibration and spatial modelling of daily ET0 in semiarid areas using Hargreaves equation. *Earth Science Informatics* **2017**.
20. Pellicer-Martínez, F.; Martínez-Paz, J.M. Grey water footprint assessment at the river basin level: Accounting method and case study in the Segura River Basin, Spain. *Ecological Indicators* **2016**, *60*, 1173–1183.
21. Giordano, R.; Pagano, A.; Pluchinotta, I.; Olivodel Amo, Rosa Hernandez, S.M.; Lafuente, E.S. Modelling the complexity of the network of interactions in flood emergency management: The Lorca flash flood case. *Environmental Modelling & Software* **2017**, *95*, 180–195.
22. García-Ayllón, S. GIS Assessment of Mass Tourism Anthropization in Sensitive Coastal Environments: Application to a Case Study in the Mar Menor Area. *Sustainability* **2018**, *10*, 1344.
23. Yang, Z.; Hsu, K.; Sorooshian, S.; Xu, X.; Braithwaite, D.; Verbist, K.M.J. Bias adjustment of satellite-based precipitation estimation using gauge observations: A case study in Chile. *Journal of Geophysical Research: Atmospheres* **2016**, *121*, 3790–3806.

24. Sorooshian, S.; Nguyen, P.; Sellars, S.; Braithwaite, D.; AghaKouchak, A.; Hsu, K., Special Publications of the International Union of Geodesy and Geophysics; Number 1, Cambridge University Press, 2014; chapter Satellite-based remote sensing estimation of precipitation for early warning systems. Extreme Natural Hazards, Disaster Risks and Societal Implications, pp. 99–112.
25. Nguyen, P.; Sellars, S.; Thorstensen, A.; Tao, Y.; Ashouri, H.; Braithwaite, D.; Hsu, K.; Sorooshian, S. Satellites Track Precipitation of Super Typhoon Haiyan. *Eos, Transactions American Geophysical Union* **2014**, *95*, 133–155.
26. Nguyen, P.; Thorstensen, A.; Sorooshian, S.; Hsu, K.; AghaKouchak, A. Flood Forecasting and Inundation Mapping Using HiResFlood-UCI and Near-Real-Time Satellite Precipitation Data: The 2008 Iowa Flood. *Journal of Hydrometeorology* **2015**, *16*, 1171–1183.
27. Karbalaee, N.; Hsu, K.; Sorooshian, S.; Braithwaite, D. Bias adjustment of infrared-based rainfall estimation using Passive Microwave satellite rainfall data. *Journal of Geophysical Research: Atmospheres* **2017**, *122*, 3859–3876.
28. Velasco-Forero, C.A.; Sempere-Torres, D.; Cassiraga, E.F.; Gómez-Hernández, J.J. A non-parametric automatic blending methodology to estimate rainfall fields from rain gauge and radar data. *Advances in Water Resources* **2009**, *32*, 986–1002.
29. Thiemig, V.; Rojas, R.; Zambrano-Bigiarini, M.; Levizzani, V.; De Roo, A. Validation of Satellite-Based Precipitation Products over Sparsely Gauged African River Basins. *Journal of Hydrometeorology* **2012**, pp. 1760–1783.
30. Ulloa, J.; Ballari, D.; Campozano, L.; Samaniego, E. Two-Step Downscaling of Trmm 3b43 V7 Precipitation in Contrasting Climatic Regions With Sparse Monitoring: The Case of Ecuador in Tropical South America. *Remote Sensing* **2017**, *9*.
31. Hill, D.J.; Baron, J. radar.IRIS: A free, open and transparent R library for processing Canada's weather radar data. *Canadian Water Resources Journal* **2015**, *40*, 409–422.
32. Zawadzki, I. On Radar-Raingage Comparision. *Journal of Applied Meteorology* **1975**, *14*, 1430–1436.
33. Freedman, D.; Pisani, R.; Purves, R. *Statistics*, 4 ed.; Viva Books, 2009.
34. Burcea, S.; Cheval, S.; Dumitrescu, A.; Antonescu, B.; Bell, A.; Breza, T. Comparision Between Radar Estimated and Rain Gauge Measured Precipitation in the Moldavian Plateau. *Environmental Engineering and Management Journal* **2012**, *11*, 723–731.
35. Pebesma, E.J. Multivariable geostatistics in S: the gstat package. *Computers & Geosciences* **2004**, *30*, 683–691.
36. Hijmans, R.J. raster: Geographic Data Analysis and Modeling, 2016.
37. Yoon, Seong-Sim amd Lee, B. Effects of Using High-Density Rain Gauge Networks and Weather Radar Data on Urban Hydrological Analyses. *Water* **2017**, *9*.
38. Scheel, M.L.M.; Rohrer, M.; Huggel, C.; Santos Villar, D.; Silvestre, E.; Huffman, G.J. Evaluation of TRMM Multi-satellite Precipitation Analysis (TMPA) performance in the Central Andes region and its dependency on spatial and temporal resolution. *Hydrol. Earth Syst. Sci.* **2011**, *15*, 2649–2663.
39. Zhang, X.; Anagnostou, E.N.; Frediani, M. Using NWP Simulations in Satellite Rainfall Estimation of Heavy Precipitation Events over Mountainous Areas. *Journal of Hydrometeorology* **2013**, *14*, 1844–1858.